Atmos. Chem. Phys., 4, 523–538, 2004
www.atmos-chem-phys.org/acp/4/523/
SRef-ID: 1680-7324/acp/2004-4-523

Atmospheric Chemistry and Physics

Inverse modeling of CO_2 sources and sinks using satellite data: a synthetic inter-comparison of measurement techniques and their performance as a function of space and time

S. Houweling[1], F.-M. Breon[2], I. Aben[1], C. Rödenbeck[3], M. Gloor[3], M. Heimann[3], and P. Ciais[2]

[1]National Institute for Space Research (SRON), Utrecht, The Netherlands
[2]Laboratoire des Sciences du Climate et de l'Environnement, Gif sur Yvette, France
[3]Max Planck Institute for Biogeochemistry, Jena, Germany

Received: 21 August 2003 – Published in Atmos. Chem. Phys. Discuss.: 20 October 2003
Revised: 10 February 2004 – Accepted: 1 March 2004 – Published: 25 March 2004

Abstract. Currently two polar orbiting satellite instruments measure CO_2 concentrations in the Earth's atmosphere, while other missions are planned for the coming years. In the future such instruments might become powerful tools for monitoring changes in the atmospheric CO_2 abundance and to improve our quantitative understanding of the leading processes controlling this. At the moment, however, we are still in an exploratory phase where first experiences are collected and promising new space-based measurement concepts are investigated. This study assesses the potential of some of these concepts to improve CO_2 source and sink estimates obtained from inverse modelling. For this purpose the performance of existing and planned satellite instruments is quantified by synthetic simulations of their ability to reduce the uncertainty of the current source and sink estimates in comparison with the existing ground-based network of sampling sites. Our high resolution inversion of sources and sinks (at $8^\circ \times 10^\circ$) allows us to investigate the variation of instrument performance in space and time and at various temporal and spatial scales. The results of our synthetic tests clearly indicate that the satellite performance increases with increasing sensitivity of the instrument to CO_2 near the Earth's surface, favoring the near infra-red technique. Thermal infrared instruments, on the contrary, reach a better global coverage, because the performance in the near infrared is reduced over the oceans owing to a low surface albedo. Near infra-red sounders can compensate for this by measuring in sun-glint, which will allow accurate measurements over the oceans, at the cost, however, of a lower measurement density. Overall, the sun-glint pointing near infrared instrument is the most promising concept of those tested. We show that the ability of satellite instruments to resolve fluxes at smaller temporal and spatial scales is also related to surface sensitivity. All the satellite instruments performed relatively well over the continents resulting mainly from the larger prior flux uncertainties over land than over the oceans. In addition, the surface networks are rather sparse over land increasing the additional benefit of satellite measurements there. Globally, challenging satellite instrument precisions are needed to compete with the current surface network (about 1 ppm for weekly and $8^\circ \times 10^\circ$ averaged SCIAMACHY columns). Regionally, however, these requirements relax considerably, increasing to 5 ppm for SCIAMACHY over tropical continents. This points not only to an interesting research area using SCIAMACHY data, but also to the fact that satellite requirements should not be quantified by only a single number. The applicability of our synthetic results to real satellite instruments is limited by rather crude representations of instrument and data retrieval related uncertainties. This should receive high priority in future work.

Correspondence to: S. Houweling
(s.houweling@phys.uu.nl)

1 Introduction

CO_2 can be considered the mobile component of the carbon cycle, since most of the exchange of carbon between the soil, ocean, and atmosphere takes place through this molecule. In addition, CO_2 is the second most important greenhouse gas in the Earth's atmosphere after water vapor. The exploitation of natural resources by mankind has increased the atmospheric CO_2 background concentration by ~30%, from 280 ppm preindustrial to 370 ppm at present. Not surprisingly, this large disturbance of the atmospheric CO_2 abundance has important consequences for climate and the carbon cycle. The increase of atmospheric CO_2 since preindustrial times is estimated to have enhanced the greenhouse

effect by 1.46 W/m^2, corresponding to 55% of the radiative forcing by all well-mixed greenhouse gases and ozone. Climatic responses to this forcing, such as temperature and precipitation changes, feed back on the carbon cycle by influencing ecosystems in various climatic zones. Increased CO_2 concentrations also directly affect vegetation, sometimes referred to as CO_2 fertilization, although the net effect on biotic carbon sequestration, in particular the role of soils, is not well understood (Prentice et al., 2001).

The combustion of fossil fuels and land use change have been identified as the major processes responsible for the observed atmospheric CO_2 increase. Together with emissions from cement production this amounts to ∼7.7–9.3 PgC/yr for the 1990s (House et al., 2003). Less than half of this amount accumulates in the atmosphere (∼3.2 PgC/yr for the 1990s), while the remainder is taken up by the land biosphere and the oceans (Prentice et al., 2001). How and where this uptake takes place is uncertain, particularly over land, and the subject of many ongoing investigations. A longer-term political motivation in this field is the international effort to reduce greenhouse gas emissions in the framework of the Kyoto Protocol on the United Nations Convention of Climate Change. By July 2003 this protocol had been ratified or acceded by 111 countries, who thereby committed themselves to a reduction of their greenhouse gas emissions over the period 2008 to 2012 by a certain percentage relative to the reference year 1990. However, the verification of these reductions, which include changes in natural reservoirs of carbon, on a national scale remains highly challenging. In summary, both from a political and a scientific point of view there is a growing need for improved CO_2 source and sink estimates on a variety of temporal and spatial scales.

The aim of this study is to explore a potentially promising recent development in this direction, that is the use of satellite observed CO_2 in conjunction with inverse modeling techniques. The underlying concept is that surface fluxes of trace gases can in principle be inferred from their atmospheric mixing ratios once it is known how they are transported through the atmosphere. In practice this implies solving an inverse problem using an atmospheric transport model. Previous studies have demonstrated the successful application of inverse modelling to this particular problem using measurements from surface networks of monitoring stations (Enting et al., 1995; Rayner et al., 1999; Bousquet et al., 2000; Gurney et al., 2002; Peylin et al., 2002; Rödenbeck et al., 2003b). The spatial and temporal resolution of these estimates, however, remained limited because of the ill-posedness of this problem and the limited number of available measurements.

Recently, several CO_2 measuring satellite instruments have appeared on stage that may potentially offer an important alternative source of many additional data. The first space-based measurements from which CO_2 concentrations can be retrieved were performed by NOAA-TOVS (Smith et al., 1979). Recent studies (Chédin et al., 2002, 2003) indicate that the NOAA-TOVS-retrieved seasonality and growth rate of CO_2 are in fair agreement with high precision surface observations by NOAA/CMDL (Conway et al., 1994) and aircraft measurements (Matsueda et al., 2002). SCIAMACHY (Bovensmann et al., 1999) and AIRS (Aumann and Pagano, 1994) are presently in orbit and the possibility to retrieve CO_2 from their instruments is being tested. Although all these instruments measure spectral intervals that contain CO_2 absorption bands, none of them was originally designed to monitor CO_2. Currently, it is investigated what a next generation of greenhouse gas, or even CO_2-dedicated instruments should look like. Such theoretical studies (like this study) led, for example, to the OCO concept currently developed for launch in 2007 (http://oco.jpl.nasa.gov/).

A number of articles have been published characterizing existing and planned instruments, retrieval methods, and associated uncertainties (Dufour and Breon, 2003; Engelen et al., 2001; Chédin et al., 2002, 1998; Kuang et al., 2002) mainly on theoretical considerations (with the exception of Chédin et al., 2002) since it is still too early for publicly available data archives. Other studies used these results to estimate the potential benefit of satellite measurements for source/sink quantification, in particular the precision that would be required for this approach to become as or even more powerful than the current surface networks (Rayner and O'Brien, 2001; Rayner et al., 2002; Pak and Prather, 2001; Patra et al., 2003). A common message is that the overall precision, including uncertainties from instrument calibration, noise, and uncertain atmospheric properties, needs to be better than 1% (or 3.6 ppm). This poses major, if not unrealistic, challenges to the instruments that are currently in orbit.

This study takes a next step by systematically comparing the potential benefits of different types of satellite instruments. For this purpose, we distinguish between thermal infrared (AIRS) and near infrared (SCIAMACHY, OCO) spectrometers. In addition, the potential advantage of a sunglint tracking near infrared instrument (OCO) is investigated. As another important difference with previous studies we solve for surface fluxes at a rather high resolution ($8° \times 10°$). This allows us to investigate where satellite measurements would be particularly useful and at which temporal and spatial scales. The different measurement techniques are expected to vary in their ability to resolve various scales. We address the interesting question how these scales compare and to what extent the instruments might complement each other.

First we will explain the applied inversion procedure, transport model, and details of the inversion set-up (Sect. 2.1). Then we will outline the assumed characteristics of the measurement instruments that will be compared (Sect. 2.2). Section 3.1 presents geographically varying uncertainty reductions of sources and sinks as gained by the inversion procedure by using simulated data from the satellite instruments and the ground network. The scale dependence of these estimates is investigated in Sect. 3.2. Subsequently, the implications of these results will be discussed (Sect. 4).

Finally, we summarize the main outcome and give recommendations for future work (Sect. 5).

2 Method

2.1 Inversion set-up

The statistical method that is generally adopted in atmospheric inverse modelling, including this study, is based on Bayes Theory (see e.g. Tarantola, 1987; Rödenbeck et al., 2003b). In short, a set of predefined parameters **x** is fitted to a set of measurement data **d** by solving a least squares cost-function $\mathcal{J}$ defined as,

$$\mathcal{J}(x) =< \mathbf{A}.\mathbf{x}-\mathbf{d}, \mathbf{C}_d^{-1}(\mathbf{A}.\mathbf{x}-\mathbf{d}) > + \\ < \mathbf{x}-\mathbf{x}_{apr}, \mathbf{C}_{\mathbf{x}apr}^{-1}(\mathbf{x}-\mathbf{x}_{apr}) >, \quad (1)$$

where <> denotes an inner product. For our particular problem the elements of **x** represent monthly surface–atmosphere fluxes of CO_2 for each surface grid box of our transport model, and $\mathbf{x}_{apr}$ contain first guess (or a priori) estimates of these fluxes. The exception to this are fossil fuel emissions, that are not estimated per month and grid, but by a single scaling factor of the a priori emissions. $\mathbf{C}_d$ and $\mathbf{C}_{\mathbf{x}apr}$ are the covariance matrices of, respectively, the vectors **d** and $\mathbf{x}_{apr}$. The atmospheric transport can be represented by a linear operator **A** quantifying the sensitivity of the measurements towards the sources and sinks (also referred to as response functions). In this study we are mainly interested in the uncertainty of the estimated fluxes, represented by the curvature of the cost-function at its minimum. Therefore the posterior flux covariance matrix $\mathbf{C}_x$ can readily be derived by taking the second derivative of the cost-function with respect to **x**, yielding

$$\mathbf{C}_x = (\mathbf{A}^T\mathbf{C}_d^{-1}\mathbf{A} + \mathbf{C}_{\mathbf{x}apr}^{-1})^{-1}. \quad (2)$$

Throughout this paper we will show differences between prior and posterior flux uncertainties, that will be quantified by the fractional change in flux uncertainty F defined as

$$F = \sigma_x/\sigma_{\mathbf{x}apr}, \quad (3)$$

where the σ's are obtained by integrating their corresponding covariance matrices over certain regions and time intervals. In addition, the quantity $1-F$ is used, which is called flux uncertainty reduction, or simply uncertainty reduction.

The elements of **A** have been computed using the global off-line Transport Model 3 (TM3) by Heimann and Körner (2003) (see also Gurney et al. (2002), and Rödenbeck et al. (2003a)). All transport model simulations were performed at a spatial resolution of $8^\circ \times 10^\circ$ (latitude$\times$longitude) and 9 vertical pressure levels from the surface to the top of the atmosphere. These computations are based on 6 hourly reanalyzed meteorological fields provided by the National Center for Environmental Prediction (NCEP) (Kalnay et al., 1996) for the year 1989 that were interpolated for use in TM3. The advective transport is calculated using the "slopes scheme" of Russell and Lerner (1981). The sub-grid scale convective air mass fluxes are evaluated using the cloud scheme of Tiedtke (1989), including entrainment and detrainment in updrafts and downdrafts. Turbulent vertical transport is based on stability-dependent vertical diffusion (Louis, 1979). Note that in our inversions of satellite observations the vector **d** contains column averaged mixing ratios. These are obtained by averaging the transport model calculated vertical profiles of CO_2 concentrations $c(p)$ using

$$d(x)_{sat} = \int_{p_{surf}}^{0} \rho(p)c(x,p)\partial p / \int_{p_{surf}}^{0} \rho(p)\partial p. \quad (4)$$

The vertical weighting function $\rho(p)$ represents the altitude dependent sensitivity of the instrument to CO_2, which is a characteristic of the applied measurement technique (see Sect. 2.2).

The a priori assumed release and uptake of carbon by the terrestrial biosphere has been derived from results of the Carbon-Cycle Model Linkage Project (CCMLP) model intercomparison (McGuire et al., 2001). We calculated a "climatological" year of Net Biome Productivity (NBP) representative of the late 1980's by averaging 10 years of model results for the "S3" scenario of the 4 participating biosphere models, resulting in a seasonally varying global distribution with a globally integrated uptake of 0.98 PgC/yr. The spatially and temporally explicit variance of this estimate is taken as a proxy of prior uncertainty, summing up to σ=0.85PgC/yr globally. Note that the CCMLP models do not simulate diurnal cycles of CO_2 exchange, although this is expected of minor importance here. The ocean uptake is based on a global inventory of ΔpCO_2 measurements by Takahashi et al. (1999) using the wind speed dependent gas transfer coefficients by Wanninkhof (1992). This approach leads to a global ocean uptake of 2.2 PgC/yr, to which we assign global uncertainty of 0.5 PgC/yr based on the combined O_2–CO_2 budget method (Prentice et al., 2001). It has been assumed that the reported global uncertainties for ocean and land represent a multi-year time scale, meaning that they do not account for inter-annual variability. For the land this time scale has been set to 10 years, consistent with the method that was used to derive the global uncertainty from the CCMLP data. For the oceans it has been set somewhat arbitrarily to 4 years, motivated by the fact that oceans are expected to exhibit a smaller inter-annual variability (Le Quéré et al., 2000). The global distribution of anthropogenic CO_2 emissions from fossil fuel burning and cement production has been taken from Andres et al. (1996), scaled to a global total of 6.05±0.38 PgC/yr (Marquardt et al., 2001) for 1989.

Local prior uncertainties (per region and month) were decomposed from global uncertainties starting with assumptions regarding their distribution and correlation in space and

time. From these assumptions a covariance matrix can be constructed that is scaled such that the square root of the sum of all its elements matches the assumed global standard deviation. The initially assumed uncertainty distribution and correlation were varied, leading to different results that will be compared and discussed in the next sections. The uncertainty distribution is either related to the source and sink processes that are active (process weighted or PW) or assumed to be the same everywhere (evenly weighted or EW). For the PW uncertainties over land we use the standard deviations of mean NBP for each $8^\circ \times 10^\circ$ grid box as calculated from the CCMLP results, which means that the standard deviation of the participating ecosystem models is taken as a surrogate of uncertainty. The PW uncertainties for the oceans are proportional to the absolute size of the $8^\circ \times 10^\circ$ fluxes, which means that the same relative uncertainty is assumed everywhere. Correlations of the prior flux uncertainties are either ignored, assuming uncorrelated fluxes (UC), or decay exponentially with the distance between 2 regions (spatially correlated, or SC). The spatial correlations attempt to account for the fact that ecosystems that are similar and experience similar climatic conditions are expected to behave similarly. For the SC scenario, correlation scales are derived from the combination of the cross- and autocorrelation terms of the CCMLP results for the terrestrial biosphere, and the Ocean Model Inter-comparison Project (OCMIP-2) for the oceans (Orr et al., 2001). This leads to characteristic correlation decay scales of 1250 and 2000 km for land and ocean respectively (Houweling et al., manuscript in preparation). All prior flux uncertainties are assumed to be uncorrelated in time. The calculated process weighted and space correlated uncertainties are typically 0.15 $mgC/m^2/s$ over the oceans and 2 $mgC/m^2/s$ over land (for monthly grid scale fluxes). Space correlation decreased the grid scale uncertainties by about a factor 2.5–3.

As this study deals only with synthetic data, the specific choice of prior estimates is not critical. Moreover, as can easily be verified from Eq. (2), the uncertainty reductions that we are interested in are in fact independent of the prior estimates themselves. The reason that the assumed prior estimates are nevertheless outlined here is that they explain the treatment of the prior uncertainties (which is the relevant quantity). The same is true for the measurements, meaning that only the assumed measurement uncertainties count. This implies that the same results would be obtained if we were able to replace the synthetic measurements by real measurements. With actual measurements, however, we would also obtain more reliable error statistics, which would alter our results. Note that the fluxes and flux uncertainties that are presented in the remainder of this paper exclude fossil fuel contributions, although they are accounted for in the inversions.

2.2 Measurement Instruments

This subsection describes the relevant parameters of the various instrument types that have been studied. All instruments have in common that their measurements do not enter the inversion one by one, but as averages of ensembles of measurements that fall within the same model grid box during a week. Furthermore, we do not attempt to specify any correlations of these ensembles, but simply assume that they are all uncorrelated. We emphasize that although the synthetic instruments are named after real instruments they are only rather crude representations of them, for lack of specifications that will only become available after rigorous in flight analyses.

The SCIAMACHY instrument is a polar orbiting nadir looking instrument that measures ultraviolet (UV), visible and near infrared (IR) solar radiation after reflection at the Earth's surface. As a consequence, it only measures the sunlit part of the globe. Moreover, we assume that the surface albedo over the oceans is too low to reach a sufficient signal to noise ratio, so that valid measurements can only be obtained over land. SCIAMACHY measures a footprint of $30 \times 60\,km^2$, implying that on average about 10% of the measured columns is cloud free (ACECHEM, 2001). We will assume that CO_2 retrieval will not be feasible for the remaining cloud contaminated columns. The instrument scans in across-track direction resulting in a 960 km swath. Because SCIAMACHY alternates between nadir and limb observations global coverage is achieved after ~6 days. This results typically in 20 000 measurements per month or about 15 measurements per ensemble. The expected locations of the measurements during a year are computed by a model of the satellite's orbit that takes into account the probability of clear sky measurements. The latter is computed using the cloud cover climatology of the International Satellite Cloud Climatology Project (ISCCP, Rossow et al., 1996), which provides monthly mean cloud cover on $2.5^\circ \times 2.5^\circ$. We acknowledge that the mean cloud cover is not fully appropriate to quantify the number of valid measurements as, for example, a 10% cloud cover all the time results in the same monthly mean cloud cover as three days of overcast skies followed by 27 clear days, while the number of clear sky measurements for these two extreme cases would obviously be quite different. This means that a characteristic spatial coherence of clouds is needed to determine a realistic probability of a cloud free column. To account for this we introduce an effective cloud cover (Cld_{eff}) that is related to the ISCCP climatology (Cld_{ISCCP}) by

$$Cld_{eff} = (Cld_{ISCCP})^{0.25}. \quad (5)$$

Note that this relationship does not follow from theoretical considerations, but has been derived empirically from the ISCCP data. A simulated SCIAMACHY sounding is declared clear/cloudy by random sampling assuming that the probability of a cloud free observation is equal to Cld_{eff}. For

other nearby SCIAMACHY measurements, we accounted for the coherency of cloud systems assuming a correlation length scale of 500 km. A precision of 3.6 ppm is assumed for each individual measurement. Although realistic precisions for SCIAMACHY remain subject of debate, 3.6 ppm seems rather optimistic (see e.g. Dufour and Breon, 2003). Nevertheless, we stick to this number for the standard set-up, and will present some results of sensitivity simulations at other precisions. The ensemble uncertainty is given by the single measurement uncertainty divided by the square root of the number of measurements, with a minimum of 1 ppm as a crude approximation of systematic errors. It is assumed that the retrieval makes use of the 1.6 µm absorption band of CO_2. At this wavelength we can assume that the absorption by CO_2 is height independent, which implies that the vertical weighting function is constant (Dufour and Breon, 2003) (see Fig. 1). Only total column measurements will be considered here, although some additional information from SCIAMACHY is anticipated from a combined use of nadir and limb measurements.

The OCO instrument is similar to SCIAMACHY, in the sense that it also measures solar radiation after reflection at the Earth's surface. In contrast to SCIAMACHY, however, it aims at sun-glint over the oceans. This significantly enhances the observed signal over these otherwise rather dark surfaces. As a result, it is able to perform sensitive CO_2 measurements over the oceans. In addition, the footprint of OCO is much smaller than that of SCIAMACHY ($1\times1.5\,km^2$), increasing the probability of cloud free column measurements. The swath width, however, is much narrower (10 km). Overall, it will provide a much larger number of useful measurements than SCIAMACHY. The measurement precision is assumed to be the same as for SCIAMACHY (3.6 ppm), although this may be somewhat conservative according to Kuang et al. (2002) who report achievable precisions of 0.3–2.5 ppm. Because the number of cloud-free scenes detected by OCO is relatively high, most of the ensemble measurement hit the 1 ppm floor of systematic uncertainty. This is true for 95% of the OCO measurements leading to an average ensemble uncertainty close to 1 ppm, compared with 51% for SCIAMACHY with an average ensemble uncertainty of 1.65 ppm.

The AIRS instrument is a polar orbiting nadir looking instrument that measures up-welling thermal IR radiation (3.7–15.4 µm) originating from the Earth's surface. The number of useful measurements is large in comparison with SCIAMACHY, because it can measure the entire globe independent of day light or surface albedo. As the foot print is only $13.5\times13.5\,km^2$ at nadir, the average fraction of cloud free measurements also is expected to be higher. The sensitivity of these measurements to CO_2 is height dependent and maximizes at a wave length dependent altitude. This allows CO_2 measurements over clouds by selecting wavelengths that are insensitive to the cloud covered part of the column. Each wavelength, however, has a rather limited sensitivity to CO_2 near the surface. Considering the large number of measurements we simply assume that weekly ensembles are available globally throughout the year. The precision of these ensembles is taken from Engelen et al. (2001), who reported 1 ppm for $4°\times5°$ degree and monthly averaged columns. This corresponds also to 1 ppm at $8°\times10°$ per week assuming uncorrelated uncertainties. Engelen et al. (2001) account for clouds, although the rather weak dependence of average cloud cover on their estimation error has been neglected here. The vertical weighting function for these measurements is taken from a retrieval derived averaging kernel presented by Engelen et al. (2001) (see Fig. 1 and Eq. 4). Their retrieval was based on an optimal estimation technique assuming a certain vertical profile of CO_2, temperature, and water vapor. We acknowledge that this weighting function is rather optimistic, since only a selection of channels within the total wavelength range is available for AIRS CO_2 retrieval. The experience with this instrument so far hints at a significant CO_2 signal from the top of the atmosphere down to about 500 hPa (R. Engelen, personal communication, 2003). Therefore we also consider a different weighting function that is sensitive to the upper half of the column only (see Fig. 1). The two weighting functions are considered here as lower and upper bounds to the expected AIRS performance, referred to as AIRS(L) and AIRS(U) respectively. Again only total column measurements will be considered here, although some height resolved information is expected from a retrieval that combines measurements at various wavelengths.

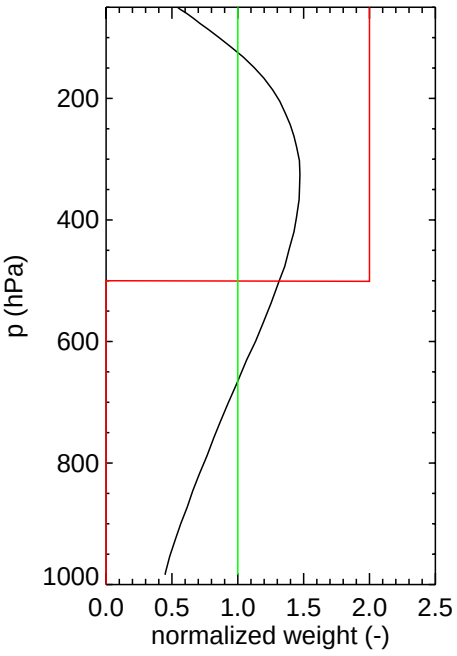

Fig. 1. Vertical weighting functions for AIRS(U) (black), AIRS(L) (red), and SCIAMACHY/OCO (green) used in this study.

The performance of the 3 instruments that are outlined above will be compared to a reference in the form of a surface flask sampling network. The size and the treatment of our network is comparable to what has been used in recent inverse modelling studies (Bousquet et al., 2000; Rödenbeck et al., 2003b). The network consists of 89 NOAA/CMDL sites including remote marine, coastal, and continental locations (Conway et al., 1994). Monthly averages of weekly flask measurements are used in the inversion. Their uncertainty is defined by the sum of the measurement uncertainty and a model representation error. The latter accounts for errors that are introduced by comparing a point measurement to a coarse model grid. The variance of the simulated concentration over a month is taken as a surrogate of this error, leading to relatively large uncertainties where large concentration gradients occur (and the largest representation errors are expected). This procedure leads to overall uncertainties of monthly measurements in the range of about 0.1 to 10 ppm (median at $\sim$0.6 ppm). Note that comparisons of model results and satellite data suffer from representation errors as well, which has been neglected in this study. These errors are expected to be somewhat less important, as the size of satellite footprints compare more favorable with the size of a model grid than the NOAA/CMDL point measurements. Moreover, the measurements within an ensemble are generally taken at different locations in the same grid box, improving the extent to which the enclosed volume is sampled.

3 Results

3.1 Geographical dependence

Inversions have been performed for all the combinations of a priori uncertainty scenarios that were described in the previous section. These combinations are: "process weighted, uncorrelated" (PW/UC), "process weighted, space correlated" (PW/SC), "evenly weighted, uncorrelated" (EW/UC), and "evenly weighted, space correlated" (EW/SC). In addition, it has been assumed that a whole year of measurements is available for each of the measurement devices SCIAMACHY, AIRS(L), AIRS(U), OCO, and the NOAA/CMDL network, thus leading to 20 inversions in total. In this section we will compare and analyze the uncertainty reductions that follow from these inversions. As can readily be seen in Eq. (2), the reduction in flux uncertainty is determined by two factors: (i) the relative uncertainties of the measurements and the prior estimates, and (ii) the sensitivity of the measured concentrations towards the fluxes, as determined by atmospheric transport. As we will see, some characteristic features of the calculated uncertainty reductions can specifically be attributed to either of these factors depending on specific conditions.

First we are interested in the uncertainty reductions gained by the different measurement concepts for PW/SC, which we consider the most realistic scenario (see Fig. 2). The blue areas in Fig. 2 point at low fractional changes in flux uncertainty, indicating that the inversion obtained uncertainty reduction is high and that the measurement system is performing well. For all satellite instruments the uncertainty reductions are larger over the continents than over the oceans, owing to the larger prior uncertainties over land. Generally, almost no uncertainty reduction is achieved for the Earth's ice caps, where the prior uncertainty is set to a very low number justified by the absence of any significant CO_2 surface exchange there. The flask network shows a more patchy uncertainty reduction pattern than the satellites, explained by the uneven sampling by the heterogeneous monitoring network. The most notable uncertainty reductions occur in grid boxes where continental measurement sites are located. Over the oceans SCIAMACHY shows by far the poorest performance of all measurement systems, resulting from the assumption that no column measurements can be retrieved from this instrument there. Measurements in sun-glint can successfully compensate for this as indicated by the results for OCO. The performance of AIRS is highly sensitive to the choice of weighting function, ranging from a performance similar to OCO for AIRS(U) to the much poorer performance for AIRS(L). Some differences between the instruments only show up for monthly uncertainty reductions (not shown). As expected, the uncertainty reductions for the sun light dependent instruments follow the latitudinally and seasonally varying in-flux of solar radiation. The thermal IR instruments show a similar seasonality in performance, which can be explained by the seasonality of its response functions (as shown in Fig.3).

Before we analyze the contributions of the right hand side terms in Eq. (2) to the fractional changes in flux uncertainty in Fig. 2, we first focus on some relevant differences between the transport matrices (**A** in Eq. 2). Figure 3 demonstrates how differences in measurement technique lead to differences in the measurement's sensitivity towards surface fluxes. AIRS(L), OCO, and NOAA/CMDL were selected because they span the range from low to high sensitivity to the surface layer. Plotted are the contributions of monthly CO_2 surface flux pulses released anywhere in the model domain to a monthly averaged measurement taken in Eastern Europe (NOAA/CMDL site "HUN" at 47° N and 17° E) in the same month as the flux pulses were released. Naturally, this response is highest near the measurement location, and decreases with the time it takes to transport (and disperse) the pulses towards this location. The more localized and intense the response, the higher the measurement's ability to resolve the local flux and, thereby, reduce its uncertainty. Ideally a satellite measurement should only be sensitive to its footprint, then after sampling the whole globe we'd be able to perfectly resolve the fluxes on the scale of the footprint. Atmospheric mixing, however, prevents this from happening. The response maximum for a surface measurement is roughly a factor of 10 higher than for a full column measurement (OCO) at the same location and is clearly more

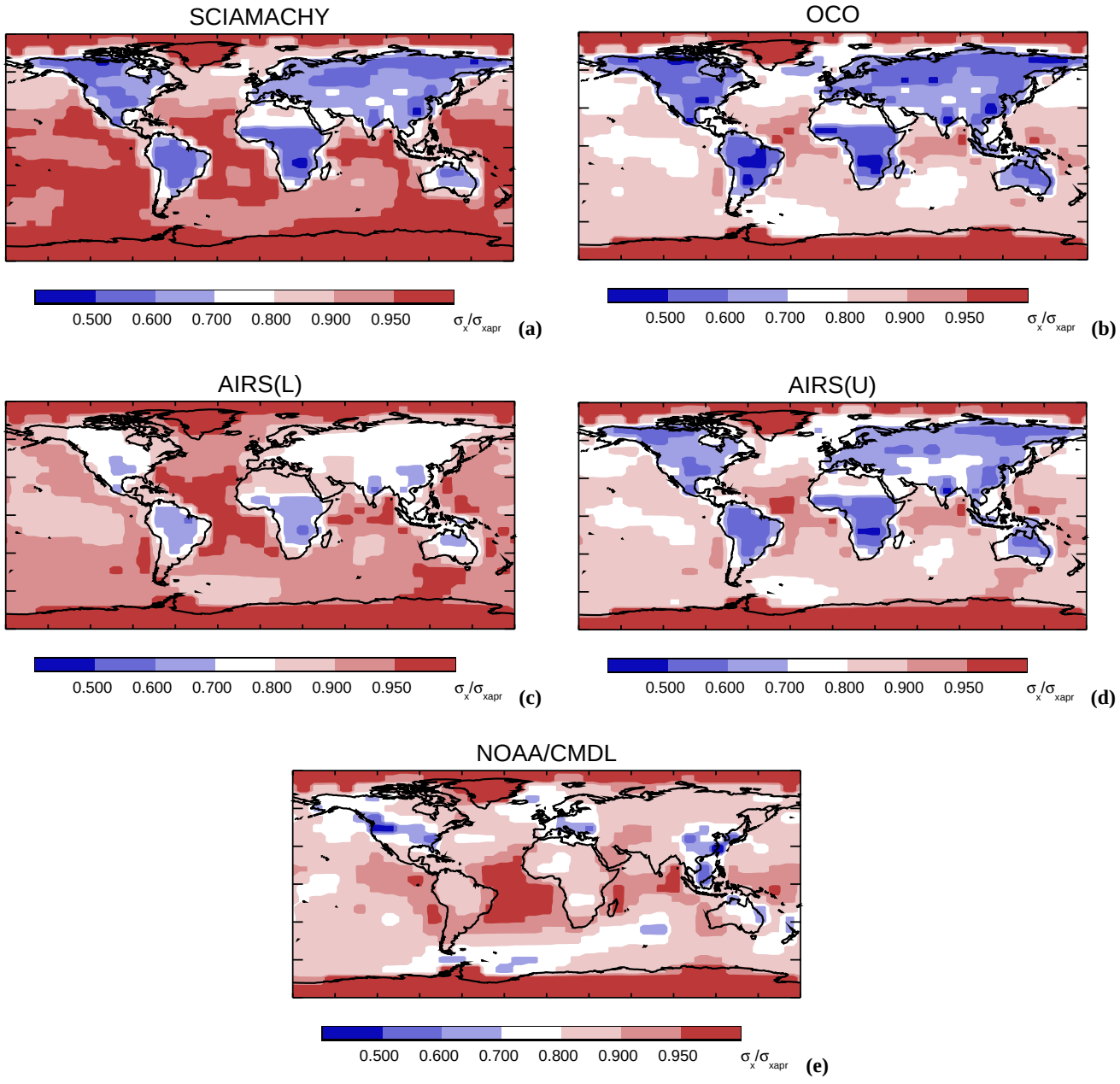

Fig. 2. Fractional change in flux uncertainty ($\sigma_x/\sigma_{\mathbf{x}pri}$) per year and per model grid cell gained by inversions on the basis of measurements by **(a)** SCIAMACHY; **(b)** OCO; **(c)** AIRS(L); **(d)** AIRS(U) **(e)** NOAA/CMDL , for process weighted and space correlated (PW/SC) prior uncertainties (see text).

localized. It implies that by measuring the total column instead of at the surface only we are less well able to resolve surface fluxes. For a full column measurement (OCO) this sensitivity is again about 10 times higher than for a measurement of only the upper half of the column (AIRS(L)). Note that, the maximum sensitivity for the latter does not occur in the same place as the measurement was taken, because that pulse is still confined to the unobserved part of the column.

As expected, the source response functions vary with atmospheric transport conditions, as illustrated in Fig. 3 by its seasonal dependence. In first instance the atmospheric mixing of the emissions is confined to a boundary layer that is shallower in winter than in summer. In our model, this results in a response function with a ∼10% higher maximum for a surface measurement in winter than in summer. The full column responses, however, are lower by ∼10% (OCO) in winter. Because the vertical weighting function

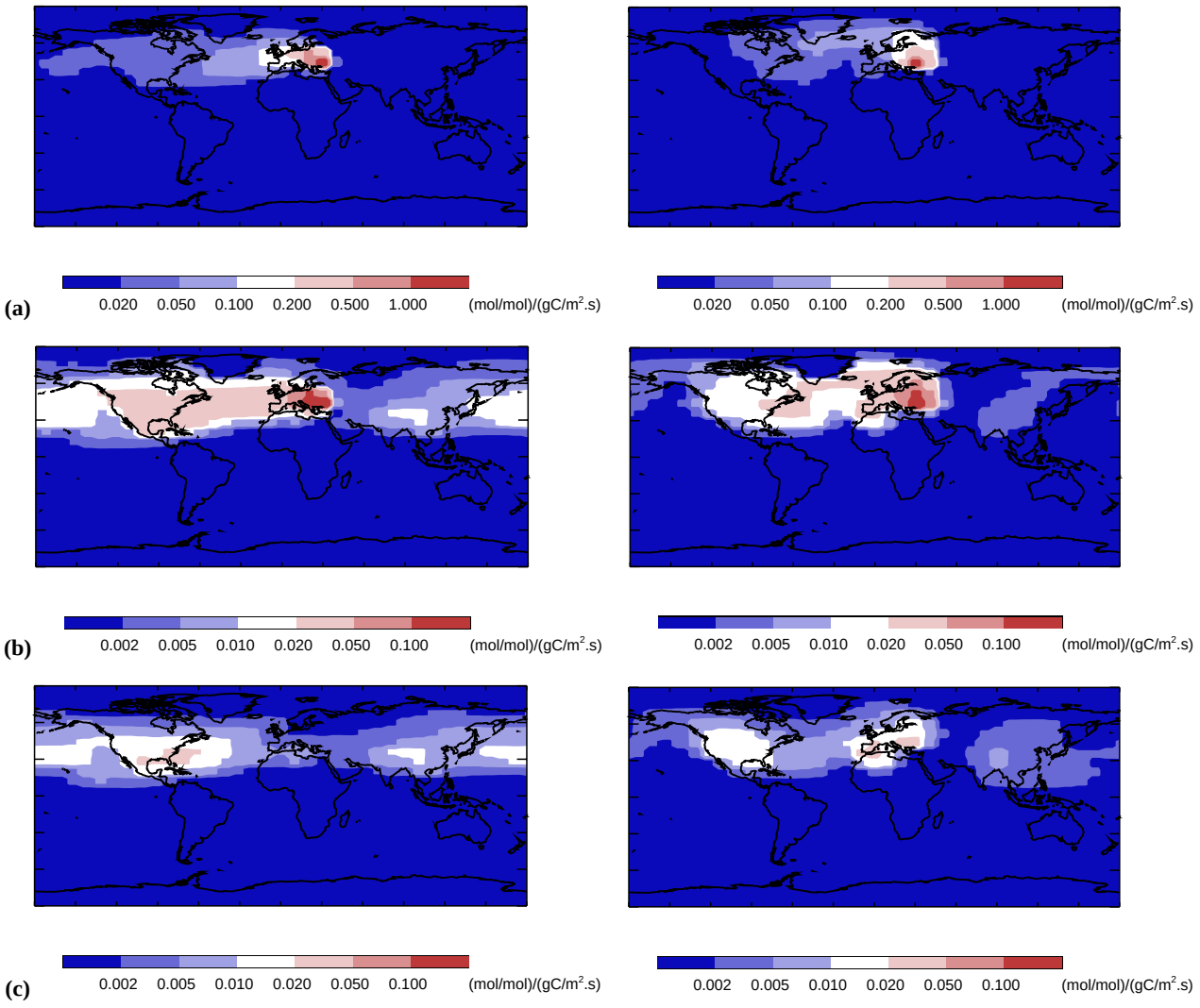

Fig. 3. The sensitivity of the concentration at NOAA/CMDL site "HUN" (47° N, 17° E) as measured by **(a)** NOAA/CMDL; **(b)** OCO; **(c)** AIRS(L) to monthly CO_2 flux pulses anywhere. The measurements refer to January (left panels), and July means (right panels). The fluxes are per grid box and are active during the same month. Note that the contour levels in panels (a) are are factor 10 higher than in panels (b) and (c).

of OCO is constant (see Fig. 1) vertical mixing only should not influence its measurements. Vertical mixing enhances the response of AIRS(L), because it transports the pulses towards observable altitudes. The reduced OCO response during winter can be explained by increased advection caused by a stronger jet-stream in winter than in summer. The response maxima of AIRS(L) in summer are clearly associated with convective activity over the United States and Europe lifting the CO_2 pulses up to observed altitudes. As expected, these areas of increased response have disappeared in winter, when continental convection has subsided.

instruments the regions of low and high uncertainty reduction are primarily determined by the prior uncertainties, and to a lesser extent by the measurement sensitivities. This is explained by the rather even measurement coverage by the satellites, as opposed to the NOAA/CMDL network where the uncertainty reduction patterns show a pronounced influence of the network configuration. Although, the measurement coverage is in fact not quite even for SCIAMACHY, this doesn't alter the patterns of uncertainty reduction much. This is because the contributions of the measurements and prior fluxes have similar large-scale patterns (distinguishing land and ocean), reinforcing each other. In other words, SCIAMACHY specifically samples those regions where we expect to be able to learn the most from additional data.

Next we will focus in more detail on the differences between the different satellite instruments. To highlight these differences we use the prior uncertainty scenario EW/UC,

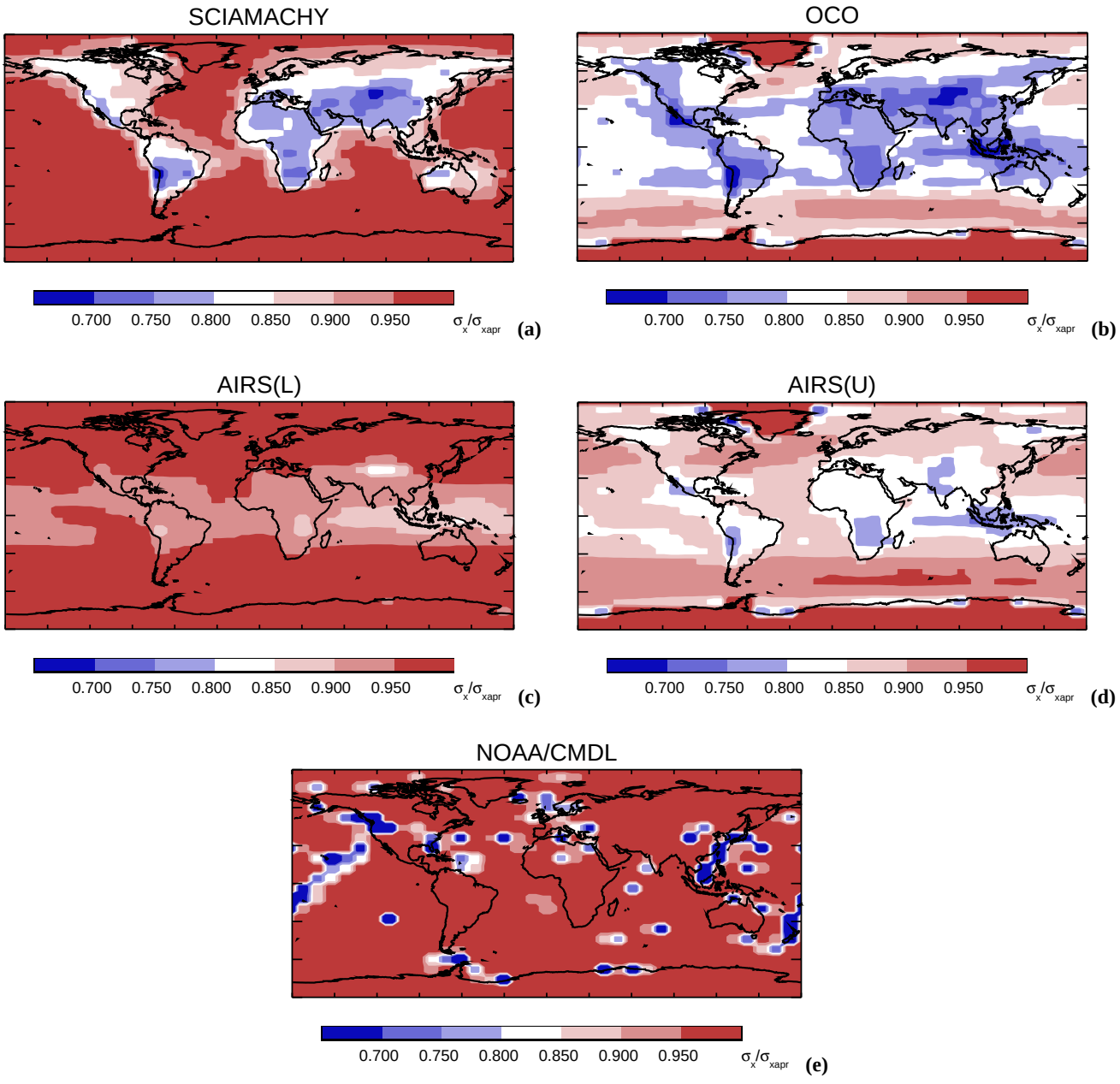

Fig. 4. As Fig. 2, but for evenly weighted uncorrelated (EW/UC) prior uncertainties.

which effectively eliminates the influence of the prior uncertainties on the uncertainty reduction patterns. Intuitively, it may seem more appropriate to use area weighted rather than evenly weighted uncertainties for this purpose. Weighting the uncertainties by area is tantamount to expressing the problem in flux units. Since the concentration data is in units of ppm this weighting has the effect of making the concentrations more sensitive to a unit change in fluxes at low latitudes than high (since low latitude grid cells are larger). Because the uncertainty reduction depends on this sensitivity, low latitude fluxes will incur a greater reduction in uncertainty for this rather trivial reason. We wish to isolate the impacts of atmospheric sampling and transport so use equally weighted uncertainties to eliminate this artifact. Figure 4 presents the uncertainty reductions for EW/UC scenario. Note that again the ice caps were kept at a low prior uncertainty, explaining why no uncertainty reduction is gained there. A notable difference with Fig. 2 is the strongly reduced land/sea contrast for AIRS and OCO. For SCIAMACHY this feature still remains, now only reflecting the lack of measurements over

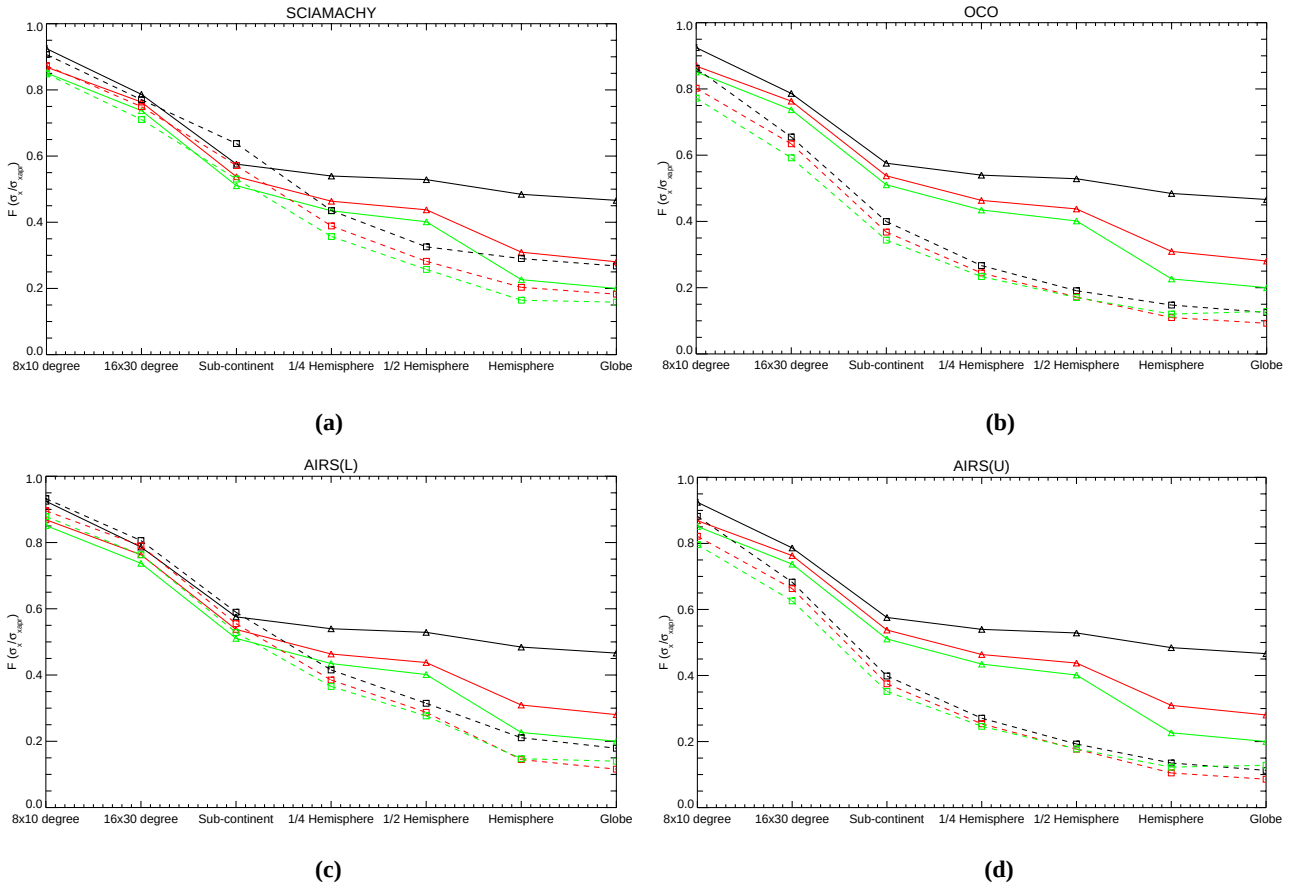

Fig. 5. Globally and annually averaged fractional change in flux uncertainty ($\sigma_x/\sigma_{\mathbf{x}pri}$) as a function of temporal and spatial scale, for **(a)** SCIAMACHY; **(b)** OCO; **(c)** AIRS(L); **(d)** AIRS(U), Green, annually integrated fluxes; red, seasonally integrated fluxes; black, monthly fluxes. Dashed and solid lines refer satellite instruments and to the NOAA/CMDL network, respectively. Prior uncertainties are process weighted and space correlated (PW/SC).

the oceans. Note that for this instrument the uncertainty reductions over the oceans are smaller compared with PW/SC, despite the fact that the oceanic prior uncertainties are larger (the globally integrated prior flux uncertainties for PW/SC and EW/UC are the same). This is explained by the fact that the prior uncertainties are now uncorrelated, while they were spatially correlated before. When using spatial correlations the uncertainty reductions are partially "shared" with neighboring fluxes, which does not happen here anymore. This effect is even more pronounced for the surface network, from which we can now clearly identify the measurement locations. Generally, areas of increased uncertainty reduction seem to be associated with increased surface elevation (e.g. Andes and Himalaya) and convection (Indonesia). Particularly in case of AIRS(L) a relationship with surface elevation makes sense, because for high enough mountains the instrument would actually see the surface. The storm tracks of the northern and southern hemisphere show up, coinciding with decreased uncertainty reductions. This can most likely be attributed to reduced responses resulting from enhanced mixing by traversing low pressure systems. We can exclude the influence of clouds, because AIRS was assumed to have a weekly measurement everywhere regardless of cloud cover. It may be surprising that also for SCIAMACHY and OCO the effects of cloud cover seem absent. This is explained by the number of measurements per weekly ensemble that is generally large enough to reduce the uncertainties to values near the assumed 1 ppm minimum (see Sect. 2.2). A consequence of this approach is that it almost eliminates the influence of variable cloud cover, which will not happen in reality. Of course, assuming the systematic error to be constant is not realistic either. This indicates the level of detail that, although relevant, we cannot properly address at present.

3.2 Scale dependence

It should be realized that the results of the previous section apply to the particular temporal and spatial scales that were selected. Here we analyze how the uncertainty reductions vary as a function of scale. For this purpose we integrated the prior and posterior uncertainties over various scales and then

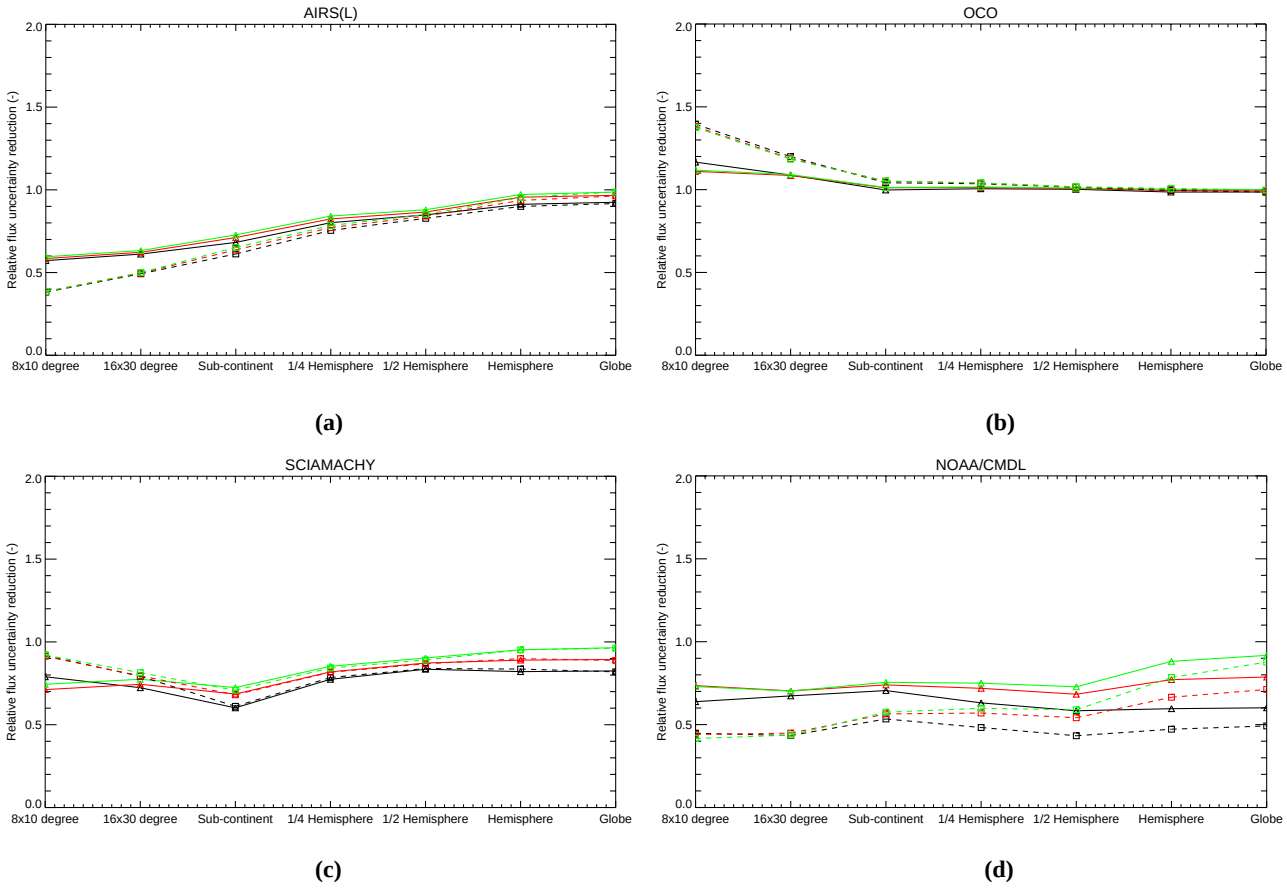

Fig. 6. As Fig. 5, expressed as uncertainty reductions relative to AIRS(U) ($[1-\sigma_x/\sigma_{\mathbf{x}pri}]_X/[1-\sigma_x/\sigma_{\mathbf{x}pri}]_{AIRS(U)}$). X refers to: Panel **(a)**, AIRS(L); panel **(b)**, OCO; panel **(c)**, SCIA; panel **(d)**, NOAA/CMDL. The solid lines show satellite results for the PW/SC scenario, dashed lines for PW/UC.

averaged the obtained uncertainty reductions over the globe and over 1 year. The selected temporal and spatial scales are: (i) monthly, seasonal, annual, and (ii) $8^\circ\times10^\circ$ (grid scale), $16^\circ\times30^\circ$ (2×3 grid cells), sub-continental, quarter Hemisphere, half Hemisphere, Hemisphere, and the Globe. The sub-continental scale refers to the 11 land and 11 ocean regions that were used in TRANSCOM 3 (Gurney et al., 2002). Contributions of the ice caps were excluded from the global averages derived at any scale. Like in the previous subsection we choose to weigh each integrated region by its number of grid cells, which was done mainly for consistency. It turns out that the choice for area or grid weighing does alter the results somewhat. In addition, the specific choice of scale and the shapes of the integrated regions affect some details of the outcome. Care is taken, however, to only interpret those aspects of the results that proved robust to such arbitrary choices.

Figure 5 shows the scale dependence of the globally and annually averaged uncertainty reduction for each instrument using PW/SC prior uncertainties. Generally, uncertainty reductions increase with scale, owing to the fact that the larger scales are observed by larger numbers of measurements and at those scales regions can better be distinguished from their neighbors (i.e. are easier to resolve). Interestingly, this applies to a lesser extent to changes in temporal than in spatial scale, suggesting that the smallest considered time scale is better resolved than the smallest spatial scale. This is true in particular for the weekly satellite measurements, except for SCIAMACHY which is due probably to contributions of oceanic regions that are poorly resolved by this instrument. For the assumed measurement uncertainties the satellites outperform the reference network on most scales. This result may not prove robust though, since, like we mentioned earlier, the measurement uncertainties for the satellites are still debated and are most likely too optimistic. The scale dependence, however, is expected to be more reliable, unless it is significantly affected by the neglect of satellite measurement correlations. We did not feel confident speculating on these correlations, and acknowledge that this factor may limit the applicability of these results.

As can be seen in Fig. 5 the decrease of the fractional change in flux uncertainty with scale has a rather similar

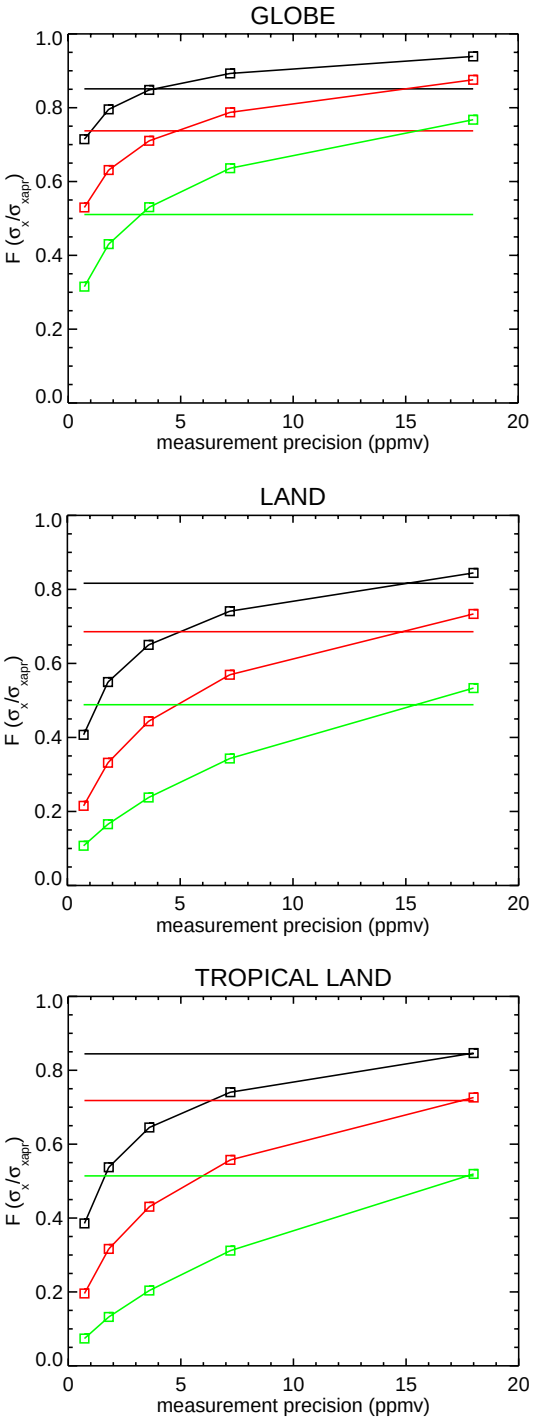

Fig. 7. Fractional change in flux uncertainty on the basis of SCIAMACHY measurements for different spatial scales as a function of measurement precision (PW/SC scenario). The uncertainties have been averaged globally and annually (top panel), over land only (middle panel), and over tropical land only (bottom panel). The scales range from $8°\times10°$ (black), $16°\times30°$ (red), to sub-continental (green). Horizontal lines indicate the corresponding uncertainties for NOAA/CMDL.

shape for all measurement systems. By plotting the ratios of uncertainty reductions for two instruments the differences become more pronounced (see Fig. 6). Values higher (lower) than 1 indicate that a given instrument is performing better (worse) than AIRS(U). We have chosen to divide by the AIRS(U) because this instrument shows a rather straight forward relation between posterior uncertainty and scale, unlike for example the surface network where the inhomogeneous sampling adds complexity to this relationship. On the global scale the performances of all satellite instruments are quite comparable, but, interestingly, they divert towards smaller scales. This is most obvious for AIRS(L) and OCO, that show respectively decreased and increased uncertainty reductions going towards smaller scales as compared with AIRS(U). Since the vertical weighting function is the main difference between these instruments, it indicates that the instruments ability to resolve smaller scales is related to its sensitivity to low altitudes.

Although the NOAA/CMDL network is more sensitive near the surface than any of the satellite instruments, its scale dependence is in fact not much different from AIRS(U). This is because the satellite instruments sample almost any location on the globe, while the surface network is at large distance of many fluxes which also reduces the corresponding sensitivities. In a comparison of AIRS(U) and NOAA/CMDL these counteracting factors largely cancel out, which is also true for SCIAMACHY and NOAA/CMDL. We tested how a smaller surface network influences this balance (not shown). Then, as expected, the performances of SCIAMACHY and AIRS improve towards smaller scales relative to the reduced surface network.

Interestingly, the relation between uncertainty reduction and scale is also influenced by the assumed correlation of the prior uncertainties as can be seen by comparing the solid and dashed lines in Fig. 6. Generally, positively correlated prior flux uncertainties reduce the scale dependence of the uncertainty reductions.

3.3 Precision requirements

Finally, we quantify the threshold uncertainty that would be needed for the SCIAMACHY instrument to outperform the current surface network, in a similar fashion as first presented by Rayner and O'Brien (2001) (see Fig. 7). In addition, the scale dependences that were presented earlier allow us to generalize this plot by showing this threshold uncertainty as a function of spatial scale. The variation of the threshold with scale turns out to be rather small, as expected from the results that were presented in the previous subsection. For the SCIAMACHY instrument the break even point for globally and annually averaged sub-continental scale fluxes is at 3–4 ppm. For the OCO instrument this threshold mixing ratio is roughly a factor 2 higher (not shown). Note that these uncertainties refer to single column measurements. In our highly simplified statistical model the uncertainties of the

weekly $8^\circ \times 10^\circ$ measurement ensembles are roughly a factor 3.5 lower. An important point to note, particularly for SCIAMACHY, is the dependence of the threshold measurement precisions on the part of the globe over which the flux uncertainty reductions were averaged. For example, by selecting only the continents the SCIAMACHY thresholds increase by about a factor of 5. A further increase of 15 to 18 ppm is obtained after selection of the tropical continents (between 30° N and 30° S). For some regions the thresholds reach even higher values, for example of 20–25 ppm over the Amazon and tropical Africa.

4 Discussion

This study confirms the conclusions by Rayner and O'Brien (2001) and Pak and Prather (2001) that rather precise satellite measurements are needed to obtain constraints on global CO_2 sources and sinks that are similar to those currently obtained from surface sampling networks. For the instruments that were tested in this study it is estimated that the required precisions are in the range of 1–2 ppm for weekly $8^\circ \times 10^\circ$ measurement ensembles and sub-continental scale fluxes. In the recent literature, measurement precisions between 0.3 and 6 ppm are reported for single column near IR measurements (Dufour and Breon, 2003; Kuang et al., 2002; Aoki et al., 2002), and 1 to 3.6 ppm for ensemble averaged thermal IR measurements (Chédin et al., 1998; Engelen et al., 2001) indicating that such requirements might be feasible. Obviously it remains to be seen how close the performance of the real instruments can get to these theoretical values. However, our analyses also indicate that regionally the required precision to match the present surface network may relax by as much as a factor of 6. Those regions are mainly located over land, because the continents are relatively poorly sampled by surface networks. This is of particular interest to carbon cycle research, because the land is generally where additional measurements are most urgently needed. As pointed out by Pak and Prather (2001), satellite measurements are expected to be particularly useful over tropical continents where the CO_2 sources and sinks are most uncertain. Because the performances of satellite instruments and the surface network maximize in different regions, added value is expected from their combined use in a single atmospheric inversion of CO_2 sources and sinks. This might work particularly well for the combination of SCIAMACHY and NOAA/CMDL network. While the first measures predominantly over the continents, with only limited measurement capability over the oceans, the opposite is true for the second. Combining different sources of measurements in an inversion, however, is not a trivial exercise because of possible differences in calibration.

Spatial and temporal resolution has been examined as another measure of satellite performance. As mentioned earlier, resolution is related to the scale dependence of the inversion-derived uncertainty reductions. Negative correlations between unresolved regions cause their sum to be relatively well constrained in comparison with the individual regions. This explains the uncertainty decrease with increasing scale that is seen, for example, in Fig. 5. The steeper the slope, the stronger the anti-correlations. If the posterior uncertainties were correlated just like the prior uncertainties, a horizontal line would be obtained at some level determined by the measurement precision. Atmospheric mixing causes the posterior fluxes to become more anti-correlated. Generally, the uncertainty reductions for the satellites decrease fairly rapidly at smaller scales, indicating that their ability to resolve small scale features is limited. Since this behavior is sensitive to the shape of the vertical weighting function, it can be concluded that by measuring the full column instead of at the surface the achievable spatial resolution is reduced. Note that our inversion set-up is not suitable for estimating the maximum achievable resolution, because we aggregated the measurements to the grid of a rather coarse resolution model. Similar limitations are introduced by the specified time discretizations. Hence we do not exploit the full information content of the measurements, in particular, on the smallest scales. It may well be, however, that by measuring total column averaged mixing ratios the achievable horizontal resolution is already lower than the size of the observational footprints. This could of course be verified using a highly resolved meso-scale atmospheric transport model. First, however, we should find out which are the relevant scales that need to be resolved to answer carbon cycle related questions. For the terrestrial biosphere these requirements seem rather stringent, since we'd ideally want to resolve the scale of ecosystems which can be much smaller than our $8^\circ \times 10^\circ$. However, given our coarse understanding in many sparsely monitored parts of the world, there is still much left to be learned on much larger scales. At this stage, full continental coverage is probably of more importance than the ability to resolve relatively small scales. This argument still favors a small footprint, because this increases the fraction of cloud free observations, and thereby spatial coverage.

Unfortunately our results do not allow a clear statement about the relative performance of near IR and thermal IR techniques. This is because of the substantial range in performance spanned by AIRS(L) and AIRS(U), indicating that its performance is in fact rather uncertain. It does, however, show that performance of the thermal IR technique is quite sensitive to the instruments ability to measure CO_2 at altitudes below 500 hPa. If this sensitivity is only modestly reduced (as in AIRS(U)) the loss in performance can be compensated by a relatively large number of measurements. It is questionable, however, to what extent thermal IR instruments will really be able to reach the surface sensitivities of AIRS(U). For example, the shortest wavelengths ($\sim$4 µm) that contribute most to the surface signal cannot be measured during daytime, because interference by reflected sunlight becomes significant (ACECHEM, 2001). On the

other hand, during nighttime the continental boundary layer is much shallower, so that the measurements should reach even lower altitudes. Again there may be additional value in combining several measurement concepts. By measuring in the near and thermal infrared we might not only be able to see the planetary boundary layer, but also measure its concentration difference with the free troposphere, which sounds highly attractive.

Our results clearly indicate that SCIAMACHY's performance is reduced by its inability to measure over the oceans. Although the instrument hasn't been designed to keep track of the sun-glint region like OCO, it does receive sporadic measurements in sun-glint. These measurements are all within a narrow latitude band near the tropics that varies seasonally. Their contribution to the instrument's overall performance will, however, not be significant, which is why they have been neglected here. Not surprisingly, the lack of ocean measurements leads to a poor performance of the atmospheric inversion over the oceans. On the $8^\circ \times 10^\circ$ scale, the estimates over land are not much influenced by this, pointing at a rather local nature of the constraints that induce the significant uncertainty reductions at this scale. Integrated over the globe, however, the benefits of ocean measurements are evident for all the analyzed scales.

A shortcoming of the presented instrument comparison is the rather crude description of measurement uncertainty. Except for the instrument's radiometric noise this is determined by the uncertainties in the retrieval of CO_2 from the measurements. The latter is influenced by knowledge on various physical and chemical properties of the measured atmospheric column. Here we have assumed that the errors will be comparable for near IR and thermal IR techniques. This may not be the case since these instruments are sensitive to atmospheric parameters that are quite different. Thermal IR measurements are sensitive to uncertain vertical profiles of temperature and humidity. For near infrared measurements, however, interference by aerosols and thin cirrus clouds are expected to be more critical. The achievable measurement precision will be determined by our ability to characterize and correct these factors. For example, it has been suggested that the effective air-mass that is sampled by a single column measurement (air-mass factor) can be quantified by measuring oxygen (O'Brien and Rayner, 2002) or, in sun-glint observations, by measuring polarized radiances (Aoki et al., 2002). The effectiveness of these procedures, however, has still to be demonstrated using real data. Another and potentially important limitation is the assumption of uncorrelated measurement uncertainties. Many instrument related uncertainties (optics, detectors, electronic circuits) and path related uncertainties (cirrus clouds, aerosols, temperature profiles), however, will likely have systematic components. This reduces the gain in precision that is obtained by co-adding or averaging large numbers of measurements. In addition, it changes the scale dependent uncertainty reductions presented in the previous section such that it reduces the increasing uncertainty reduction with increasing scale.

Last but not least it should be mentioned that the atmospheric transport model is assumed to be perfect, while obviously it isn't. In particular vertical mixing is known to vary across the models, reflecting the relatively large uncertainties that are associated with the parameterizations of convection and turbulent mixing (Denning et al., 1999). This may have important implications for satellite instruments that are sensitive to the shape of the vertical concentration profile (such as AIRS). In absence of a height dependent sensitivity, the column averaged concentrations may rather be less susceptible to transport model uncertainties than surface concentrations, as pointed out by Rayner and O'Brien (2001). Related to vertical mixing is a tendency of many transport models that use diagnosed winds (e.g. from ECMWF or NCEP) to simulate mean "ages" of stratospheric air that are much younger than the measurements indicate (Andrews et al., 2001; Jones et al., 2001). This may lead to large scale off-sets in the inversion-derived flux estimates.

5 Conclusions

We studied the potential benefit of satellite instruments that measure atmospheric CO_2 mixing ratios for the estimation of CO_2 sources and sinks by inverse modeling. Three hypothetical instrument types have been compared, inspired by currently operational and planned missions. The relative performance of these instruments is quantified by synthetic simulations of their ability to reduce the uncertainty in the current CO_2 source and sink estimates. These performances are put in perspective by comparison to the current NOAA/CMDL flask sampling network. The thermal IR instrument AIRS has the advantage of relatively high number of measurements, leading to a notably better performance over the oceans than SCIAMACHY. This shortcoming of SCIAMACHY can be compensated by measuring in sun-glint, as demonstrated by OCO. An uncertain factor of AIRS, however, is its ability to measure at low altitudes which is demonstrated to be of crucial importance. For the near IR instruments SCIAMACHY and OCO the surface sensitivity will certainly be more favorable. Overall OCO is the most promising satellite concept of those tested because it is a near IR instrument, which measures in sun-glint over the oceans. This result was obtained despite a relatively conservative precision assumption for the OCO instrument. The performance of the instruments is shown to vary geographically, as determined by the assumed prior uncertainties, measurement uncertainties, and atmospheric transport properties. Enhanced horizontal mixing reduces the performance by effectively dispersing the concentration gradients. Convection, on the contrary, is advantageous to instruments that are insensitive to the lower altitudes. Generally, the geographical differences suggest that additional benefits can be obtained from the combined use of satellite instruments and

surface networks, provided that systematic differences can be accounted for. We have shown that the instrument performances should be quantified with reference to the considered scale, as they vary as a function of temporal and spatial scale. Generally the performance improves going to larger scales, as these scales become progressively better constrained by the increasing number of measurements addressing them. Increased sensitivity near the surface increases the instruments ability to resolve smaller scales. The scale dependence of the satellite instruments is rather comparable to that of the surface network, with a slight improvement for satellites that are sensitive to the surface and reach full global coverage (OCO and AIRS(U)). In line with earlier studies, the required precision of weekly columns of CO_2 on $8^\circ \times 10^\circ$ needed to improve the inversion-derived annual flux estimates on a subcontinental scale over the whole globe is less than 1% (or 3.5 ppm) for all instruments. For OCO this requirement is a factor 2 less stringent than for SCIAMACHY (2 versus 1 ppm). The SCIAMACHY requirements, however, relax by a factor of 5 if only the continents are taken into account. We anticipate that SCIAMACHY can contribute most significantly to our estimates of CO_2 fluxes over tropical continents. This study relies heavily on the assumed precision of satellite measurements, which is poorly quantified at present. This is not only a limitation of our synthetic approach, but, unless the error assessments improve significantly, this situation will remain when real data are available. Therefore, we'd like to emphasize that a reliable uncertainty assessment is vital to any interpretation of these measurements using inverse modeling. In particular the identification of random and systematic components should receive high priority.

Acknowledgements. We acknowledge fruitful discussions within the COCO project, and are particularly grateful to R. Engelen (ECMWF) and C. Crevoisier (LMD). Further, we'd like to thank A. Maurellis and H. Schrijver (SRON) for useful support. P. Rayner and K. Gurney provided constructive and valuable reviews of this paper. This study was financially supported by the EC project COCO (EVG1-CT-2001-00056) and LSCE, with special thanks to Philippe Ciais for initiating this work.

Edited by: P. Kasibhatla

References

ACECHEM: Atmospheric composition explorer for chemistry and climate interactions, SP-1257 4, ESA, 2001.

Andres, R. J., Marland, G., Fung, I., and Matthews, E.: A $1^\circ \times 1^\circ$ distribution of carbon dioxide emissions from fossil fuel consumption and cement manufacture, 1950–1990, Global Biogeochemical Cycles, 10, 419–429, 1996.

Andrews, A. E., Boering, K. A., Wofsy, S. C., Daube, B. C., Jones, D. B., Alex, S., Loewenstein, M., Podolski, J. R., and Strahan, S. E.: Empirical age spectra for the midlatitude lower stratosphere from in situ observations of CO_2: Quantitative evidence for a subtropical "barrier" to horizontal transport, J. Geophys. Res., 106, 10 257–10 274, 2001.

Aoki, T., Aoki, T., and Fukabori, M.: Path-radiance correction by polarization observation of Sun glint glitter for remote measurements of tropospheric greenhouse gases, Applied Optics, 24, 2002.

Aumann, H. H. and Pagano, R. J.: Atmospheric infrared sounder on Earth observing system, Optical Eng., 33, 776–784, 1994.

Bousquet, P., Peylin, P., Ciais, P., Quere, C. L., Friedlingstein, P., and Tans, P. P.: Regional changes in carbon dioxide fluxes of land and oceans since 1980, Science, 290, 1342–1346, 2000.

Bovensmann, H., Burrows, J. P., Buchwitz, M., Frerick, J., Noël, S., Rozanov, V. V., Chance, K. V., and Goede, A. P. H.: SCIAMACHY: Mission objectives and measurement modes, J. Atmos. Sci., 56, 127–150, 1999.

Chédin, A., Saunders, R., Hollingsworth, A., Scott, N., Matricardi, M., Etcheto, J., Clerbaux, C., Armante, R., and Crevoisier, C.: The feasibility of monitoring CO_2 from high resolution infrared sounders, J. Geophys. Res., 108, doi:10.1029/2001JD001 443, 1998.

Chédin, A., Hollingsworth, A., Scott, N. A., Serrar, S., Crevoisier, C., and Armante, R.: Annual and seasonal variations of atmospheric CO_2,N_2O and CO concentrations retrieved from NOAA-TOVS satellite observations, Geophys. Res. Lett., 29, doi:10.1029/2001GL14 082, 2002.

Chédin, A., Serrar, S., Scott, N. A., Crevoisier, C., and Armante, R.: First global measurement of midtropospheric CO_2 from NOAA polar satellites: Tropical zone, J. Geophys. Res., 108, doi:10.1029/2003JD003 439, 2003.

Conway, T. J., Tans, P. P., Waterman, L. S., and Thoning, K. W.: Evidence for interannual variability of the carbon cycle from the national oceanic and atmospheric administration climate monitoring and diagnostics laboratory global air sampling network, J. Geophys. Res., 99, 22 831–22 855, 1994.

Denning, A. S., Holzer, M., Gurney, K. R., et al.: Three-dimensional transport and concentration of SF_6: A model intercomparison study (Transcom 2), Tellus, Ser. B, 51, 266–297, 1999.

Dufour, E. and Breon, F.-M.: Spaceborne estimate of atmospheric CO_2 column using the differential absorption method: Error analysis, Appl. Optics, 42, 3595–3609, 2003.

Engelen, R. J., Scott Denning, A., Gurney, K. R., and Stephans, G. L.: Global observations of the carbon budget, 1. Expected satellite capabilities in the EOS and NPOESS eras, J. Geophys. Res., 106, 20 055–20 068, 2001.

Enting, I. G., Trudinger, C. M., and Francey, R. J.: A synthesis inversion of the concentration and $\delta^{13}C$ of atmospheric CO_2, Tellus, Ser. B, 47, 35–52, 1995.

Gurney, K. R., Law, R. M., Denning, A. S., et al.: Towards robust regional estimates of CO_2 sources and sinks using atmospheric transport models, Nature, 415, 626–630, 2002.

Heimann, M. and Körner, S.: The global atmospheric tracer model TM3, Model description and user's manual release 3.8a, Max Planck Institute of Biogeochemistry, 2003.

House, J. I., Prentice, I. C., Ramankutty, N., Houghton, R. A., and Heimann, H.: Reconciling apparent inconsistencies in estimates of terrestrial CO_2 sources and sinks, Tellus, Ser. B, 55, 345–363, 2003.

Jones, D. B. A., Andrews, A. E., Schneider, H. R., and McElroy, M. B.: Constraints on meridional transport in the stratosphere imposed by the mean age of air in the lower stratosphere, J. Geophys. Res., 106, 10 243–10 256, 2001.

Kalnay, E., Kanamitsu, M., Kistler, R., et al.: The NCEP/NCAR 40-year reanalysis project, Bull. Am. Met. Soc., 77, 437–471, 1996.

Kuang, Z., Margolis, J., Toon, G., Crisp, D., and Yung, Y.: Spaceborn measurements of atmospheric CO_2 by high-resolution NIR spectrometry of reflected sunlight: An introductory study, Geophys. Res. Lett., 29, doi:10.1029/2001GL014 298, 2002.

Le Quéré, C., Orr, J. C., Monfray, P., Aumont, O., and Madec, G.: Interannual variability of the oceanic sink of CO_2 from 1979 through 1997, Global Biogeochem. Cycles, 14, 1247–1265, 2000.

Louis, J. F.: A parametric model of vertical eddy fluxes in the atmosphere, Boundary Layer Meteorol., 17, 187–202, 1979.

Marquardt, W., Brüggemann, E., Auel, R., Herrmann, H., and Möller, D.: Trends of pollution in rain over East Germany caused by changing emissions, Tellus, Ser. B, 53, 529–545, 2001.

Matsueda, H., Inoue, H. Y., and Ishii, M., Aircraft observations of carbon dioxide at 8–13 km altitude over the western Pacific from 1993 to 1999, Tellus, Ser. B, 54, 2–20, 2002.

McGuire, A. D., Sitch, S., Clein, J. S., et al.: Carbon balance of the terrestrial biosphere in the twentieth century: Analysis of CO_2, climate and land use effects with four process-based models, Global Biogeochem. Cycles, 15, 183–206, 2001.

O'Brien, D. M. and Rayner, P. J.: Global observations of the carbon budget, 2. CO_2 column from differential absorption of reflected sunlight in the 1.61 μm band of CO_2, J. Geophys. Res., 107, doi:10.1029/2001JD000 617, 2002.

Orr, J. C., Maier-Reimer, E., Mikolajewicz, U., Monfray, P., Sarmiento, J. L., Toggweiler, J. R., Taylor, N. K., Palmer, J., Gruber, N., Sabine, C. L., Le Quéré, C., Key, R. M., and Boutin, J.: Estimates of anthropogenic carbon uptake from four three-dimensional global ocean models, Global Biogeochem. Cycles, 15, 43–60, 2001.

Pak, B. C. and Prather, M. J.: CO_2 source inversions using satellite observations of the upper troposhere, Geophys. Res. Lett., 28, 4571–4574, 2001.

Patra, P. K., Sasano, S. M. Y., Nakajima, H., and Inoue, G.: An evaluation of CO_2 observations with SOFIS sensor for surface source inversion, J. Geophys. Res., 2003.

Peylin, P., Baker, D., Sarmiento, J., Ciais, P., and Bousquet, P.: Influence of transport on annual mea and seasonal inversions of atmospheric CO_2 data, J. Geophys. Res., 107, doi:10.1029/2001JD000 857, 2002.

Prentice, I. C., Farquhar, G., Fashm, G., Goulden, M., Heimann, M., Jaramillo, V., Kheshgi, H., Le Quéré, C., and Scholes, R. J., The carbon cycle and atmospheric carbon dioxide, in Climate Change 2001: The scientific basis, edited by J. T. Houghton, Y. Ding, D. J. Griggs, M. Noguer, P. J. van der Linden, X. Dai, K. Maskell, and C. A. Johnson, pp. 183–237, Cambridge University Press, 2001.

Rayner, P. J. and O'Brien, D. M.: The utility of remotely sensed CO_2 concentration data in surface source inversions, Geophys. Res. Lett., 28, 175–178, 2001.

Rayner, P. J., Enting, I. G., Francey, R. J., and Langenfelds, R.: Reconstructing the recent carbon cycle from atmospheric CO_2, $\delta^{13}CO_2$ and O_2/N_2 observations, Tellus, Ser. B, 51, 213–232, 1999.

Rayner, P. J., Law, R. M., O'Brien, D. M., Butler, T. M., and Dilley, A. C.: Global observations of the carbon budget 3. initial assessment of the impact of satellite orbit, scan geometry, and cloud on measuring CO_2 from space, J. Geophys. Res., 107, doi:10.1029/2001JD000 618, 2002.

Rödenbeck, C., Houweling, S., Gloor, M., and Heimann, M.: Time-dependent atmospheric CO_2 inversions based on interannually varying transport, Tellus, Ser B, 55, 488–497, 2003a.

Rödenbeck, C., Houweling, S., Gloor, M., and Heimann, M.: CO_2 flux history 1982–2001 inferred from atmospheric data using a global inversion of atmospheric tracer transport, Atmos. Chem. Phys., 3, 1919–1964, 2003b.

Rossow, W. B., Walker, A. W., Beuschel, D. E., and Roiter, M. D.: International Satellite Cloud Climatology Project (ISCCP) documentation of new cloud datasets, Tech. Rep. WMO/TD-No. 737, World Meteorological Organization, 1996.

Russell, G. and Lerner, J.: A new finite-differencing scheme for the tracer transport equation, J. Appl. Meteorol., 20, 1483–1498, 1981.

Smith, W. L., Woolf, H. M., Hayden, C. M., Wark, D. Q., and McMillin, L. M.: The TIROS-N operational vertical sounder, Bull. Amer. Meteor. Soc., 60, 1177–1187, 1979.

Takahashi, T., Wanninkhof, R. H., Feely, R. A., et al.: Net sea-air CO_2 flux over the global oceans: An improved estimate based on the sea-air pCO_2 difference, in 2nd International Symposium, CO_2 in the Oceans, extended abstracts, pp. 18–01, Center Global Env. Res., Tsukuba, Japan, 1999.

Tarantola, A.: Inverse Problem Theory, Methods for Data Fitting and Model Parameter Estimation, Elsevier, New York, 1987.

Tiedtke, M.: A comprehensive mass flux scheme for cumulus parameterization in large-scale models, Mon. Weather Rev., 117, 1779–1800, 1989.

Wanninkhof, R.: Relationship between wind speed and gas exchange, Geophys. Res. Lett., 26, 7373–7382, 1992.